ANALYTICAL METHOD FOR SEISMIC PERFORMANCE EVALUATION OF INFILLED R/C FRAMES

Maidiawati[1] and Yasushi Sanada[2]
[1]Graduate student, Graduate School of Engineering, Toyohashi University of Technology, Japan
Email: m109103@edu.imc.tut.ac.jp, sanada@arch.eng.osaka-u.ac.jp
[2]Associate Prof. Osaka University, Japan

ABSTRACT

According to several studies that masonry infills have significant effect on the response of reinforced concrete (R/C) frame structures subjected to seismic action. This paper presents a simple analytical method for evaluating the seismic performance of a masonry infilled R/C frame structure. In this model, masonry inifll is replaced by a diagonal compression strut which is represented by distributed compression transferred diagonally between infill/frame interfaces. Infill/frame contact length can be determined by solving two equations, i.e., static equilibriums related to compression balance at infill/frame interface and lateral displacement compatibility. Consequently, strut width is presented as a function of infill/frame contact length. The infill contribution and infilled frame seismic performances are evaluated based on evaluated infilled/frame contact length and strut width of infill. The validity of the analytical model is verified by comparing to experimental results of several brick masonry infilled R/C frames, which represented a typical R/C building with nonstructural masonry elements in Indonesia. As a result, good agreement is shown between experimental and analytical results on the performance curve of the infill frame including lateral stiffness and strength.

KEY WORDS: Infill/frame contact length, Masonry infill, Seismic performance, r/c frame, Strut width.

1. INTRODUCTION

Reinforced concrete frames with a masonry infill as a partition wall are common in developing countries with high seismicity. However, the presence of a masonry infill is usually neglected in seismic design calculations of building structures, assuming it to be a nonstructural element. Extensive research works have been carried out to in order to predict the effect of masonry infill to structural behavior of RC frame as reported by Mehrabi et al (1996), Murty (1996), Decanini et al (2004), Hashemi and Mosalam (2007), Bahran and Sevil (2010). Analytical and experimental studies of the authors also showed that a masonry infill contributes significantly to the seismic performance of this kind of structure (Maidiawati et al., 2008 and 2011).

This paper proposes an analytical method for seismic performance of infilled R/C frame structures affected by masonry infill. The infill contribution was evaluated based on a strut model. In this study, a masonry infill is replaced by a diagonal compression strut, which represents a distributed compression transferred diagonally between infill/frame interfaces. The infill/frame contact length can be determined by solving two equations, i.e., static equilibriums related to the compression balance at infill/frame interface and lateral displacement compatibility. Consequently, the equivalent strut width is presented as a function of infill/frame contact length.

A series of reversed cyclic lateral loading test on bare frame and brick masonry infilled frame structures was conducted to verify the proposed analytical method. Experimental specimens represented a typical R/C building with brick masonry elements in Indonesia. This paper compares experimental results and numerical simulations using the proposed method.

2. MODELING OF INFILLED FRAMES

This study targets a brick masonry infilled R/C one-bay frame with a fixed base and a rigid beam, as shown in Figure 1a, representing a multi-story infilled frame where beam flexural deformation is constrained by the infill. Contact/separation is caused between the bounding column and infill under column flexural deformation and infill shear deformation, as shown in Figure 1a. The following analytical model and results of masonry infill contribution have been partially reported in Maidiawati et al (2012).

The masonry infill wall was replaced by a diagonal compression strut having the same thickness and material properties as the infill panel. In this model, however, a compression stress block at the infill/frame interface was replaced by an equivalent rectangular block, as shown in Figure 1b, where the averaged compressive strength, f_m', was given for the infill strength. f_m' was evaluated by multiplying the uniaxial compressive strength of infill, f_m, by a reduction factor, α, which resulted in a value of approximately 0.65 in the calculations described below. As a result, the compression strut was represented by a force that was distributed uniformly symmetrically along the diagonal axis of the infill. The lateral distribution force along the column height, which acts on the bottom of the compressive column, is given by Equation 1.

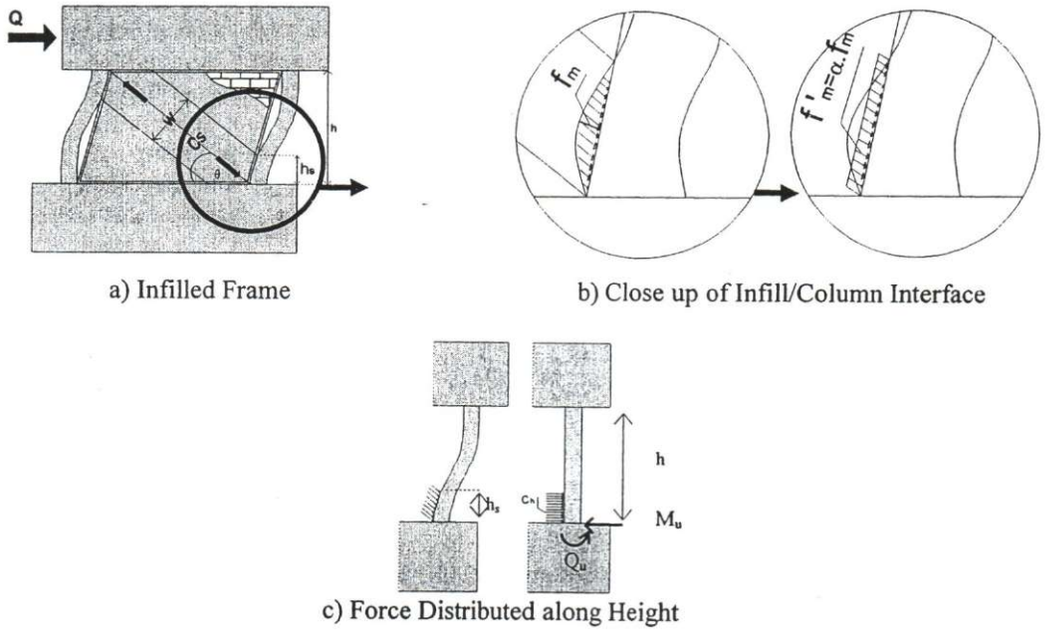

a) Infilled Frame

b) Close up of Infill/Column Interface

c) Force Distributed along Height

Figure 1. Modeling of masonry-infilled frame

$$C_h = t\, f_m^{'} \cos^2\theta \qquad (1)$$

In which, C_h: uniformly distributed force along column height, as shown in Figure 1c, t: thickness of infill, θ: inclination angle of strut, as shown in Figure 1a.

Assuming that the column on the compressive side (right side in Figure 1a) yields in flexure at the bottom, the moment distribution along column height, ${}_cM(y)$, is obtained with Equations 2. Yield moment, however, is calculated with Equation 3 based on the JBDPA standard (2005).

In the case of $0 \le y \le h_s$

$${}_cM(y) = {}_{y=0}M_u - Q_u y + 1/2 C_h y^2 \qquad (2a)$$

In the case of $h_s \le y \le h$

$${}_cM(y) = {}_{y=0}M_u - Q_u y + C_h h_s y - 1/2\, C_h h_s^2 \qquad (2b)$$

$$M_u = 0.8\,a_t\,\sigma_y D + 0.5\,N\,D\left(1-\frac{N}{b\,D\,F_c}\right) \quad (3)$$

where, h_s: infill/column contact height, as shown in Figure 1(c), h: column height, as shown in Figure 1c, M_u: flexural strength of column, Q_u: shear force at column bottom, which is determined with Equation 5, a_t: total cross-sectional area of tensile reinforcing bars, σ_y: yield stress of longitudinal reinforcement, D: column depth, N: axial force, b: column width, F_c: compressive strength of concrete. However, the axial force at the bottom of the column was calculated as a summation of building weight (initial axial load), N_a, axial force due to shearing force in the beam, N_b, and vertical component of the strut force, $C_v h_s (=t\,f_m' \cos\theta \sin\theta\, h_s)$, as shown in Figure 2.

Lateral displacement along column height, ${}_c\delta(y)$, is produced by double integrals of Equation 2, which is shown by Equation 4.

In the case of $0 \le y \le h_s$

$${}_c\delta(y) = \frac{1}{EI}\left(1/24 C_h y^4 - 1/6 Q_u y^3 + 1/2 M_u y^2\right) \quad (4a)$$

In the case of $h_s \le y \le$ h

$${}_c\delta(y) = \frac{1}{EI}\begin{pmatrix}(1/6 C_h h_s - 1/6 Q_u) y^3 + \\ (1/2 M_u - 1/4 C_h h_s^2) y^2 + \\ 1/6 C_h h_s^3\, y - 1/24\, C_h h_s^4\end{pmatrix} \quad (4b)$$

where, EI: bending stiffness.

In Equations 2 and 4, Q_u is given by Equation 5 when assuming a rotation of zero at the column top.

$$Q_u = \frac{2M_u}{h} + C_h h_s - \frac{C_h h_s^2}{h} + \frac{C_h h_s^3}{3h^2} \quad (5)$$

On the other hand, lateral deformation along infill height, ${}_i\delta(y)$, is defined by Equation 6, assuming uniform shear strain, ${}_i\theta$. Therefore, intersection height between column and infill can be evaluated by solving Equation 7, as shown in Figure 3. The figure shows that intersection height should equal h_s. The unknown h_s was obtained iteratively after satisfying Equation 7. In this study, the Newton Raphson method was used to find h_s. The procedure above is presented in the flowchart in Figure 4.

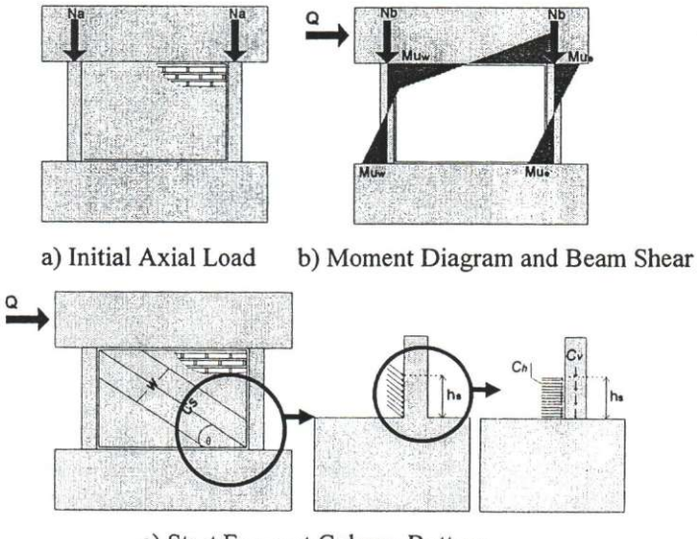

a) Initial Axial Load b) Moment Diagram and Beam Shear

c) Strut Force at Column Bottom

Figure 2. Evaluation axial force at column bottom

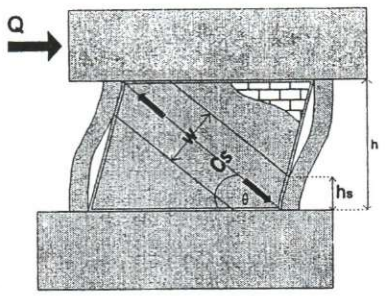

Figure 3. Lateral displacement compatibility along column height

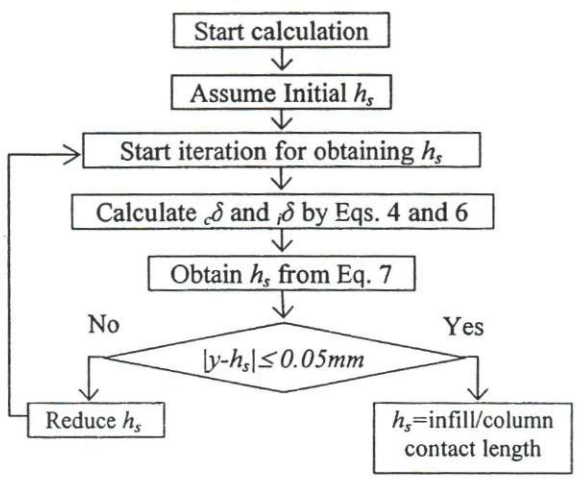

Figure 4. Flowchart for identifying infill/column contact length

$$ {}_i\delta(y) = {}_i\theta\, y = \frac{{}_c\delta(y=h)}{h} y \tag{6} $$

$$ {}_c\delta(h_s) = {}_i\delta(h_s) \tag{7} $$

The width of compression strut, which is shown in Figure 3, is determined as a function of infill/column contact height by Equation 8.

$$ w = 2h_s \cos\theta \tag{8} $$

The diagonal compression strut caused on infill, C_s, was evaluated based on the strut widths obtained by Equation 8 as given in Equation 9. Ultimate lateral strength, V_m, of the infill is given in Equations 10.

$$ C_s = w\, t\, f_m' \tag{9} $$

$$ V_m = C_s \cos\theta \tag{10} $$

On the other hand, the ultimate lateral strength of infilled frame, Q, was evaluated by Equation 11. Where, Q_u is ultimate shear force at the bottom of compressive column as shown in Figure 5b obtained by Equation 5, $Cs/2\ cos\ \theta$ is shear force at lower beam caused by strut force, and Q_t, is shear force at bottom of tensile column as shown in Figure 5a.

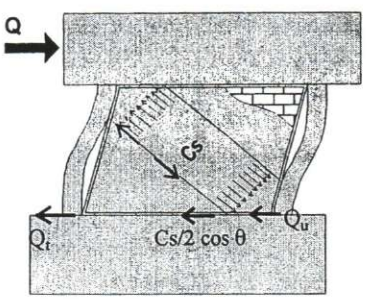

a) Infilled Frame

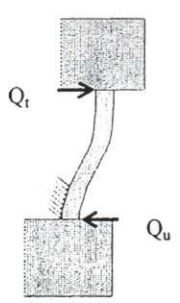

b) Compressive Column

Figure 5. Shear force evaluation of infilled frame

$$ Q = Q_u + C_s / 2 \cos\theta + Q_t \tag{11} $$

3. EXPERIMENT FOR VERFICATION

To clarify the validity of the proposed method experimentally, a series of structural tests was conducted on R/C frames with/without a brick masonry infill. The specimens represented a partial frame of a typical R/C building, as shown Photo 1 and Figure 6, which was investigated in

detail by the authors after the 2007 Sumatra earthquakes, Indonesia (Maidiawati and Sanada, 2008). The following experimental program and results have been partially reported in Maidiawati et al. (2011) with the exception of two specimens with infill consisting of scaled bricks.

Photo 1. Referential building damaged by the 2007 sumatra earthquakes

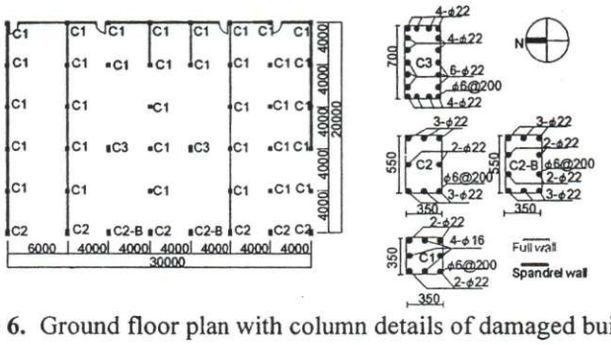

Figure 6. Ground floor plan with column details of damaged building

3.1. Test Specimens

BF Specimen

Four 1/2.5 scale RC one-bay frame specimens were prepared: one bare frame (BF) and three infilled frames with masonry bricks (IF_FB, IF_SBw/oFM and IF_SB described in the following). Table 1 summarizes the combination of test parameters. Figure 7 shows the configuration and bar arrangements of the BF specimen. The mechanical properties of specimens are shown in Table 2.

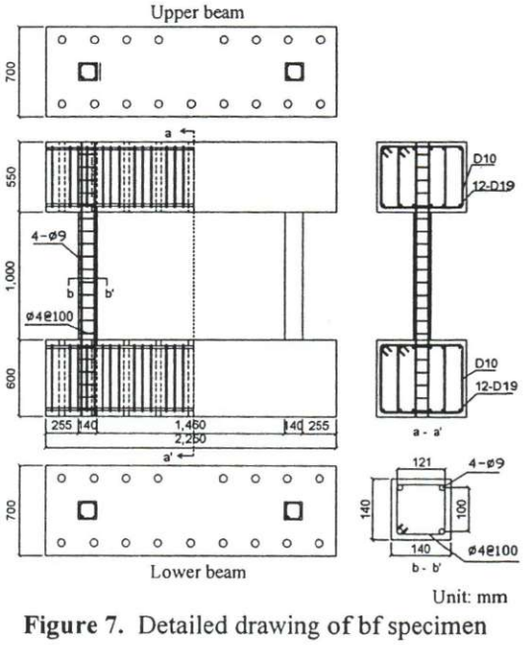

Figure 7. Detailed drawing of bf specimen

Table 1. Parameters for specimens

Specimens	Column	Experimental parameters	
		Brick wall	Plaster
BF	cross-section: 140x140 main bar: 4-Ø9 hoop: 2-Ø4@100	none	none
IF_FB		thickness: 100 mm	20 mm (each side)
IF_SBw/oFM		thickness: 44 mm	none
IF_SB		thickness: 44 mm.	8 mm (each side)

IF_FB Specimen

IF_FB specimen had a full-scale brick infill, which was extracted from the referential building, as shown in Photo 2a. It was transported to Toyohashi University of Technology, Japan, and was installed in the IF_FB specimen, as shown in Photo 2b. Mortar was applied between the bounding frame and inserted wall with material properties as shown in table 2.

a) Extracting of wall

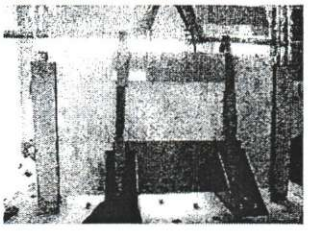

b) Installation of brick wall

Photo 2. Preparation of IF_BF specimen

Table 2. Material properties

Concrete		
Specimen	Compressive strength	Tensile strength
	N/mm²	N/mm²
BF	19.6	1.89
IF_FB	20.6	1.96
IF_SBw/oFM	26.6	1.90
IF_SB	27.3	1.98
Mortar		
Specimen	Compressive strength	Tensile strength
	N/mm²	N/mm²
IF_FB (only for boundaries)	40.8	3.33
IF_SBw/oFM	44.7	2.33
IF_SB	48.6 (for infill) 42.9(for finishing)	3.26 (for infill) 2.89 (for finishing)
Masonry prism		
Specimen	Compressive strength (f_m)	Tensile strength
	N/mm²	N/mm²
IF_FB	2.91	0.25
IF_SBw/oFM	16.3	2.3
IF_SB	18.5	2.3
Reinforcing bar		
Bar number	Yield strength	Tensile strength
	N/mm²	N/mm²
9 (BF, IF_FB)	355	440
4 (BF, IF_FB)	583	631
9 (IF_SBw/oFM, IF_SB)	338	382
4 (IF_SBw/oFM, IF_SB)	497	778

IF_SBw/oFM and IF_SB Specimens

IF_SBw/oFM and IF_SB specimens had a scaled brick infill consisting of 1/2.5 scale bricks having dimensions of 88 mm in length, 44 mm in width and 20 mm in height. Although the compressive strength of the scaled bricks made in Japan was arranged to be similar to that of Indonesian bricks, the masonry prisms with mortar beds exhibited higher strengths for IF_SBw/oFM and IF_SB specimens from material tests, as shown in Table 2. Finishing mortar with a thickness of 8 mm was applied only to the wall surfaces of IF_SB specimen, which resulted in an infill thickness of 44 mm and 60 mm for IF_SBw/oFM and IF_SB, respectively. Figure 8 is a detailed drawing of the IF_SB specimen.

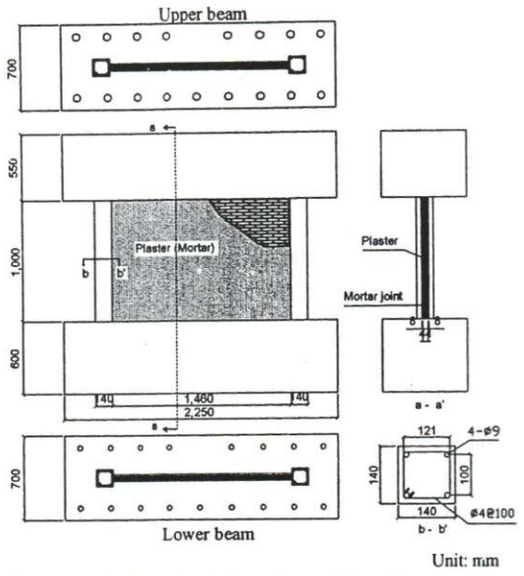

Figure 8. Detailed drawing of IF_SB specimen

3.2 Test Method

The specimens were subjected to a constant vertical load of 183.4 kN (≈ 0.24 x column sectional area x compressive strength of concrete) based on the estimated weight of the upper floors. Then, reversed cyclic lateral loads were applied to the specimens. Incremental loads were controlled by drift angle, *R* (rad.), ratio of lateral displacement to column height. The lateral loading program had an initial cycle to R=1/800 followed by two cycles to R=1/400, 1/200, 1/100, 1/50, 1/25 and 1/12.5 for BF and IF_FB specimens, and an initial cycle to R=1/400 followed by two cycles to R=1/200, 1/100, 1/50, 1/25 and 1/12.5 for IF_SBw/oFM and IF_SB specimens, respectively.

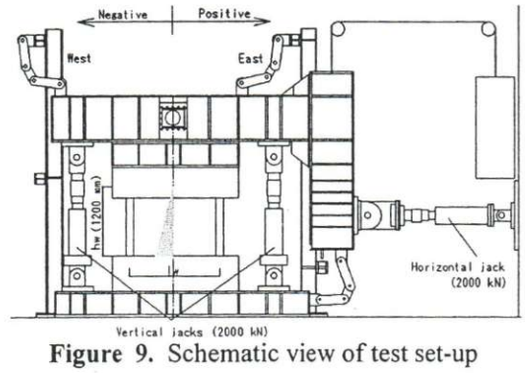

Figure 9. Schematic view of test set-up

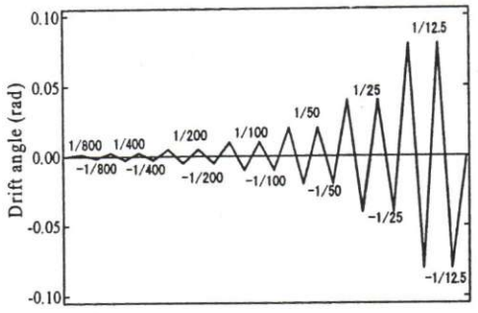

Figure 10. Lateral loading history for BF and IF_FB

When the specimens failed, loading was stopped. The schematic representation of the experimental set-up and the lateral loading history are shown in Figures 9 and 10, respectively. The shear span to depth ratio (= h_w/l_w illustrated in Figure 9) of the specimens was maintained at 0.75 throughout the tests so that lateral loads were applied at an assumed second floor height of 1200 mm.

3.3 Test Result and Discussion

Figure 11 compares lateral force vs. drift ratio, R, relationships between the specimens. The maximum lateral strength of 36.8 kN was observed at 2.0% for the BF specimen. On the other hand, the maximum strengths reached 174.0 kN, 174.75 kN and 257.25 kN at 0.5%, 0.25% and 0.23% drift ratios for IF_FB, IF_SBw/oFM, and IF_SB, respectively. The deformation capacity, which was defined as a deformation where post-peak strength dropped to 80% of peak strength, was 2.8% for BF, whereas they decreased to 1.6%, 1.0% and 0.5% for IF_FB, IF_SBw/oFM, and IF_SB, respectively.

The infill contribution was extracted by evaluating the difference between lateral forces of infilled frame and bare frame at each load step (at the same drift ratio), as shown in Figure 12. In this study, the envelope curves were simulated according to the proposed analytical method as follows.

4. VERIFICATION OF ANALYTICAL METHOD.

According to the analytical method proposed in this study, infill/frame contact lengths, h_s, were evaluated to be 312 mm, 259 mm, and 218 mm for IF_FB, IF_SBw/oFM and IF_SB, respectively. The ultimate strength of infill, V_m, were 112.6 kN, 164.3 kN and 214.7 kN for IF_FB, IF_SBw/oFM and IF_SB, respectively which were evaluated by Equations 10. Initial lateral stiffness of infill was determined by Equation 12, where, E_m is elastic modulus of infill of inifll (=750f_m') based on Paulay and Priestley (1992). The evaluated lateral strength and lateral stiffness of infill are compared to the experimental results as shown in Figure 12.

$$K = \frac{E_m w t}{d} \cos^2 \theta \qquad (12)$$

According to Equation 11, the ultimate lateral strength of infilled frame can be predicted and compared to experimental results as shown in Figure 13. In which, initial stiffness of infilled frame, K_{IF}, was identified by Equation 13 with the assumption that the compatible lateral displacement between column top and wall infill at yielding deformation. Good agreement was obtained between experimental and analytical results until strength began to drop after peaking. It was verified that the proposed method could be used reasonably for estimating the seismic performance of a masonry infilled frame.

$$K_{IF} = \frac{E_m w t}{d} \cos^2 \theta \frac{Q}{V_m} \qquad (13)$$

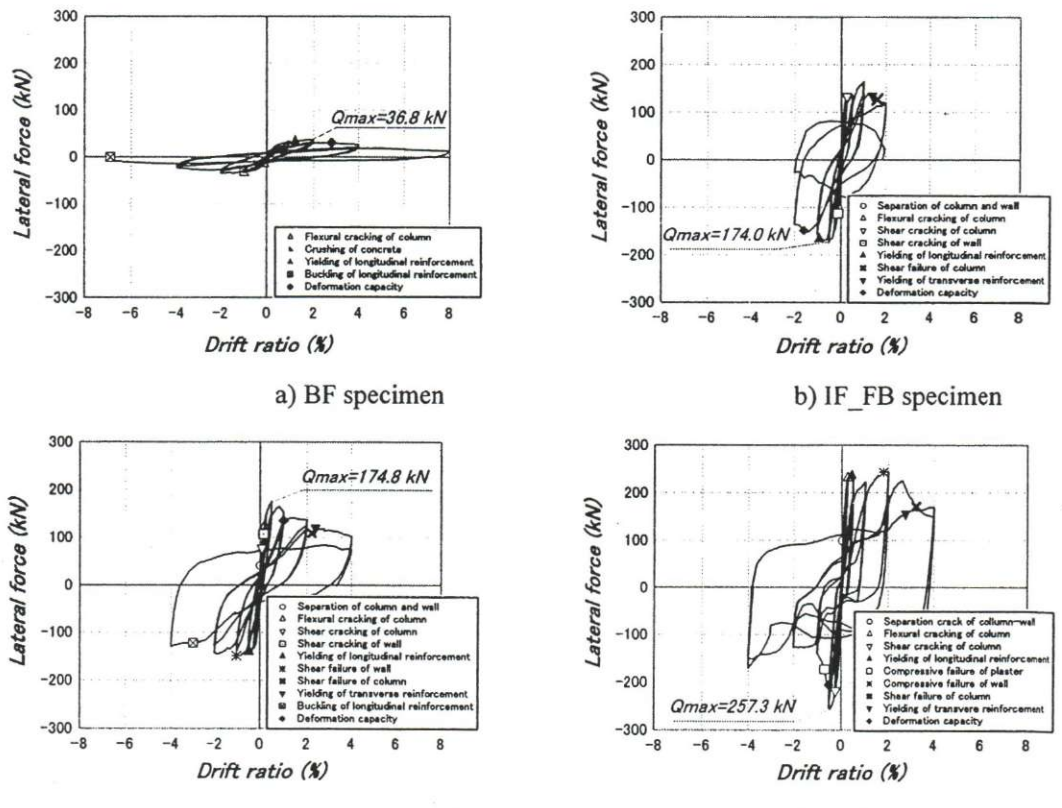

Figure 11. Lateral force–drift ratio relationships of infilled frames obtained from test

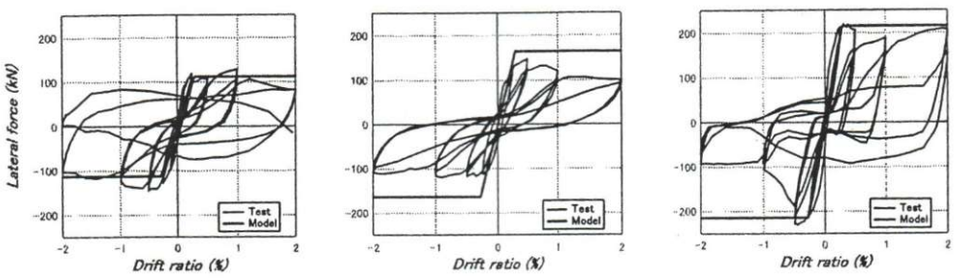

a) IF_FB specimen b) IF_SBw/oFM specimen c) IF_SB specimen

Figure 12. Lateral force-drift ratio relationship of infill

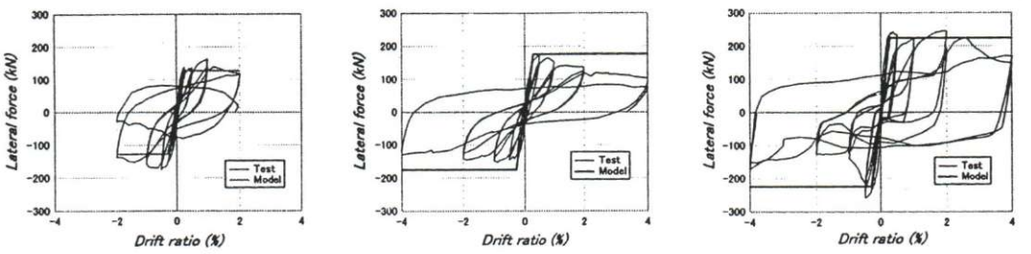

a) IF_FB specimen b) IF_SBw/oFM specimen c) IF_SB specimen

Figure 13. Comparison of performance curves of infilled frame

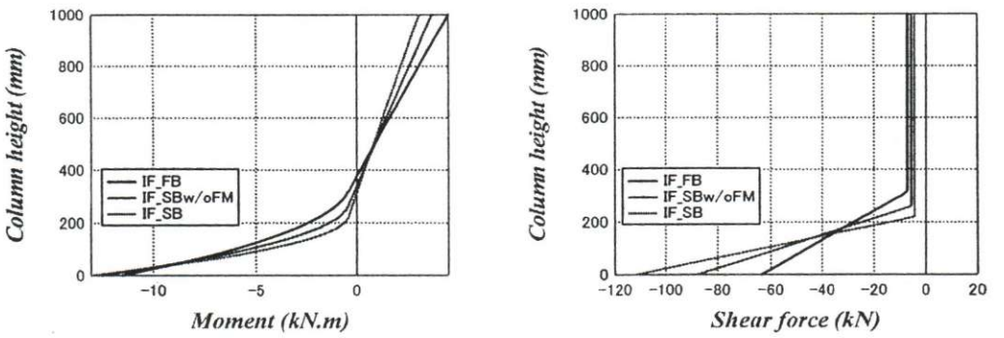

Figure 14. Stress diagrams of column

Moreover, the proposed method can identify distributions of bending moment and shear force along the column height, as shown in Figure 14. Bending moments at the base of the column were 11.5 kN.m, 12.6 kN.m and 13.1 kN.m for IF_FB, IF_SBw/oMF and IF_SB, respectively. Shear forces at the column bottom were 63.6 kN, 87.8 kN and 111.9 kN for IF_FB, IF_SBw/oMF and IF_SB, respectively. Compared to the moment of 10.5 kN.m and shear force of 21.0 kN for BF, it was found that the masonry infill increased not only the strength of the overall frame, but also local bending moment and shear force acting on the column. Therefore, the deformation capacities of infilled frame specimens were much lower than that of the bare frame specimen.

5. CONCLUSIONS

A simplified analytical method based on diagonal strut model was proposed to evaluate the infill contribution on seismic performance of infilled R/C frame structure. In this model, a compression strut was replaced by a uniformly distributed force along the diagonal direction on an RC frame. The compression strut width was determined based on contact length between column and infill which was evaluated by solving static equilibriums and lateral displacement compatibility. The lateral strength and stiffness of infilled frame were determined according to evaluated infilled/frame contact length and strut width of infill.

A series of structural test was conducted for verification. The performance curve of the infill framed in the experimental specimens was simulated by the proposed method. Consequently, good agreement is shown between experimental and analytical results. It is verified that the proposed method could be used reasonably for estimating the seismic performance of a masonry infilled frame.

It was also identified that an infill can increase local bending moment and shear force at bounding columns, which seemed to decrease the deformation capacities of bounding columns.

6. ACKNOWLEDGEMENTS

This study was supported financially by Housing Research Foundation (Jusoken), Japan, and Indonesian Ministry of Higher Education

REFERENCES

Baran M., and Sevil T., (2010). Analytical and Experimental Studies on Infilled Rc Frames. *International Journal of The Physical Science*. 5(13), 1981-1998.

Decanini L., Mollaioli F., Mura A., Saragoni R., (2004). Seismic Performace of Masonry Infilled Frames. *Procedding of 13th World Conference on earthquake Engineering,* Vancouver, B.C., Canada.

Hashemi A. and Mosalam K. M (2007). Seismic Evaluation of Reinforced Concrete Building Including Effect of Masonry Infill Walls. *PEER Report 2007/100. University of California, Berkeley.*

Maidiawati and Sanada Y. (2008). Investigation and Analysis of Buildings Damaged during the September 2007 Sumatra, Indonesia Earthquakes. *Journal of Asian Architecture and Building Engineering.* 7(2),371–378.

Maidiawati, Sanada Y, Daisuke Konishi, and Jafril Tanjung. (2011). Seismic Performance of Nonstructural Brick Walls Used in Indonesian R/C Buildings. *Journal of Asian Architecture and Building Engineering.* 10(1),203-210.

Maidiawati, Sanada Y., and Thandar Oo. (2012). A Simple Approach for Determining Contact Length between Frame and Infill of Brick Masonry Infilled

Mehrabi A., Benson Shing P., Schuller M., and Noland J., (1996). Experimental Evaluation of Masonry-Infilled RC Frames. *Journal of Structural Engineering.*122 (3), 228-237

Murty C. V. R., (1996). Effect of Brittle Masonry Infill on Displacement and Ductility Demand of Moment Resisting Frames. *Proceeding of Eleventh World Conference on Earthquake Engineering, Acapulco, Mexico.*

R/C Frames. *Proceeding of 15th World Conference on Earthquake Engineering, Lisboa, Portugal.*

T. Paulay, M.J.N. Priestley. (1992). *Seismic Design of Reinforced Concrete and Masonry Buildings*. John Wiley & Sons, Inc., New York, USA. ISBN 0-471-54915-0.

The Japan Building Disaster Prevention Association (JBDPA). (2005). *Standard for Seismic Evaluation of Existing Reinforced Concrete Buildings*, 2001. English Version,1st.